

## Supporting information

# Uniform Zn Deposition Achieved by Ag coating for Improved Aqueous Zinc Ion Batteries

*Qiongqiong Lu<sup>†,\*</sup>, Congcong Liu<sup>†</sup>, Yehong Du<sup>#</sup>, Xinyu Wang<sup>#,\*</sup>, Ling Ding<sup>†</sup>, Ahmad Omar<sup>†</sup>, Daria Mikhailova<sup>†,\*</sup>*

<sup>†</sup>Leibniz Institute for Solid State and Materials Research (IFW) Dresden e.V., Helmholtzstraße 20, 01069 Dresden, Germany.

<sup>#</sup> Institute of Materials and Technology, Dalian Maritime University, Dalian 116026, China

**Correspondence:** q.lu@ifw-dresden.de (Q.Q. Lu) wangxinyu@dlmu.edu.cn (X.Y. Wang)  
d.mikhailova@ifw-dresden.de (D. Mikhailova)

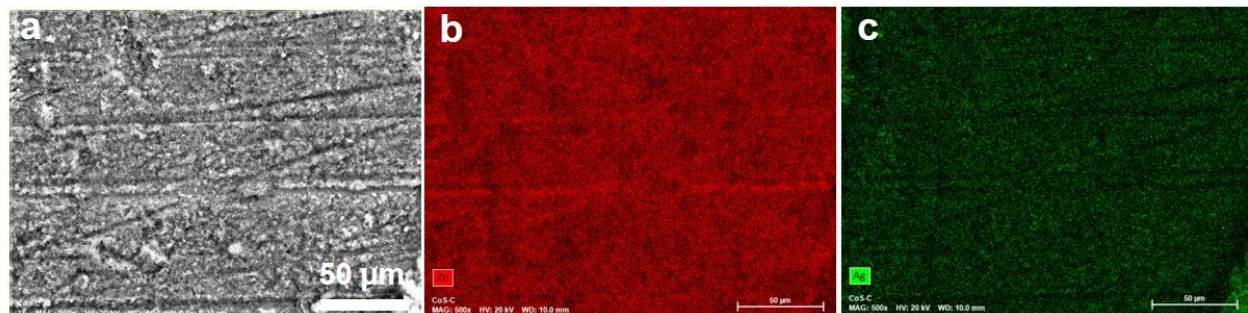


**Figure S1.** a) SEM image of Ag-Zn; b) Zn and c) Ag elemental mapping of the Ag-Zn electrode.

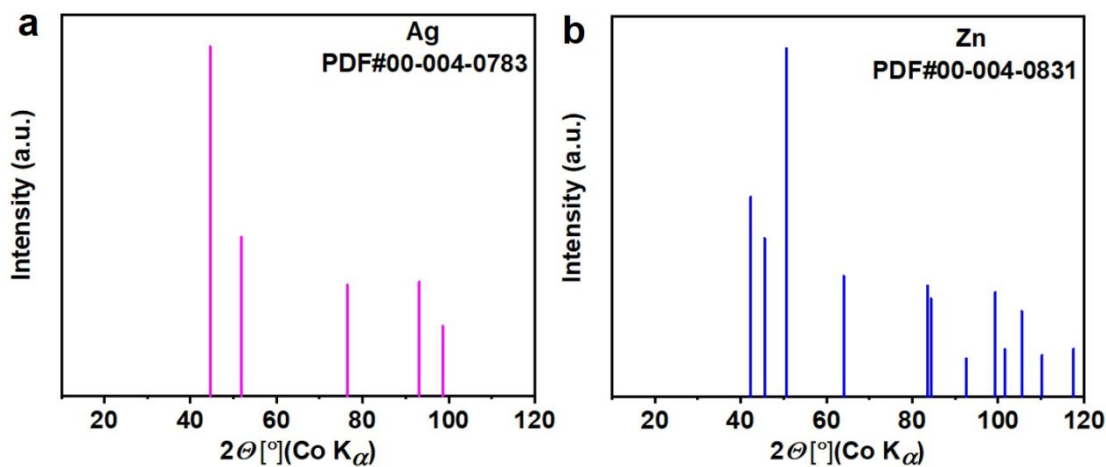


**Figure S2.** Reference XRD patterns of a) Zn and b) Ag.

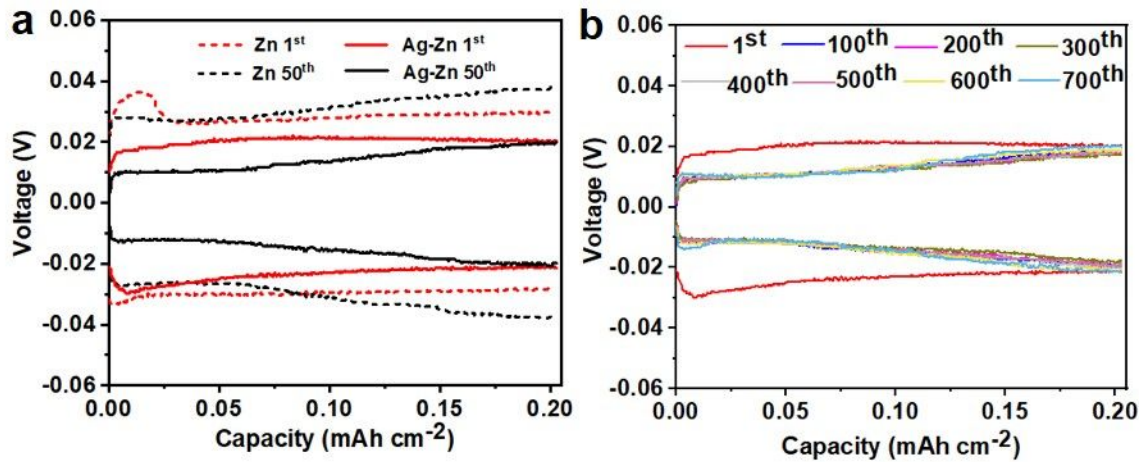


**Figure S3.** a) Discharge/charge curves of Zn plating/stripping for untreated Zn and Ag-Zn at 1<sup>st</sup> and 50<sup>th</sup> cycle at 0.2 mA cm<sup>-2</sup>. b) Discharge/charge curves of Zn plating/stripping for Ag-Zn at different cycles at 0.2 mA cm<sup>-2</sup>.

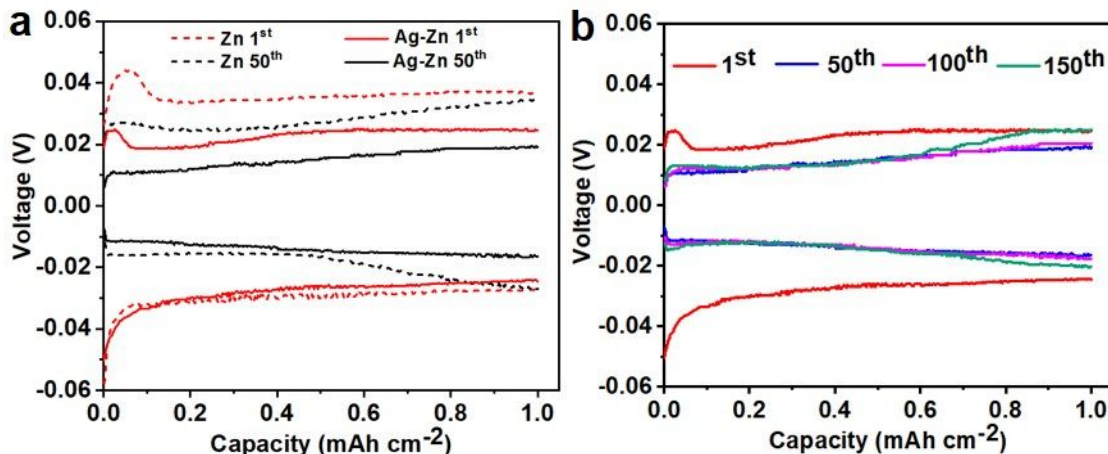


**Figure S4.** a) Discharge/charge curves of Zn plating/stripping for untreated Zn and Ag-Zn at 1<sup>st</sup> and 50<sup>th</sup> cycle at 1 mA cm<sup>-2</sup>. b) Discharge/charge curves of Zn plating/stripping for Ag-Zn at different cycles at 1 mA cm<sup>-2</sup>.

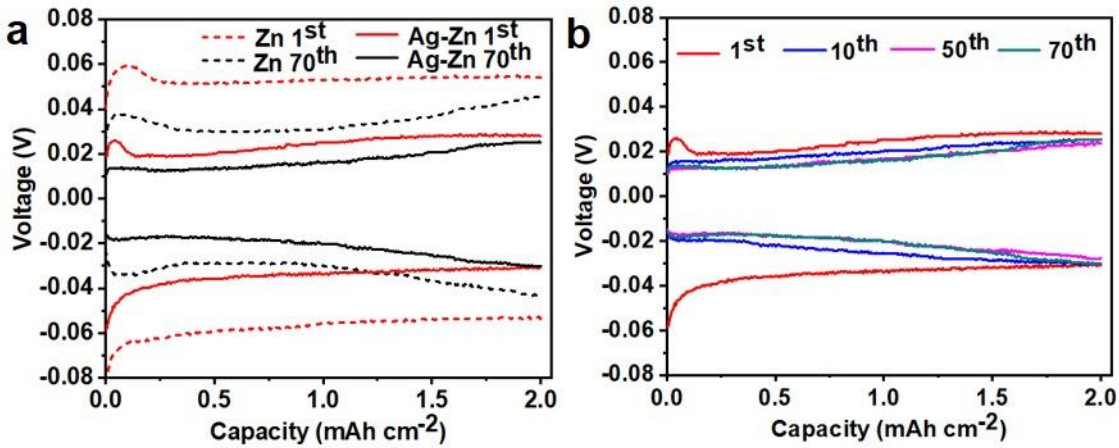


**Figure S5.** a) Discharge/charge curves of Zn plating/stripping for untreated Zn and Ag-Zn at 1<sup>st</sup> and 70<sup>th</sup> cycle at 2  $\text{mA cm}^{-2}$ . b) Discharge/charge curves of Zn plating/stripping for Ag-Zn at different cycles at 2  $\text{mA cm}^{-2}$ .

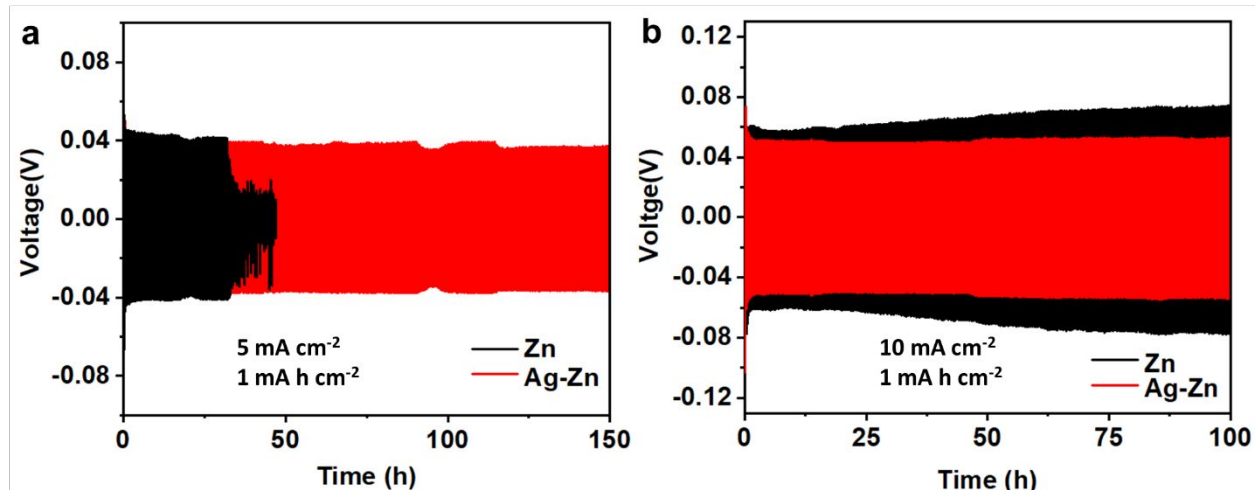


**Figure S6.** Cycling performance of symmetric cells at current density of a) 5  $\text{mA cm}^{-2}$  b) 10  $\text{mA cm}^{-2}$  with a capacity of 1  $\text{mA h cm}^{-2}$ .

**Table S1.** Comparison of the performance of symmetric cells with recent literature works on various Zn metal protective strategies.

Protective layers	Current density (mA cm <sup>-2</sup> )	Capacity (mAh cm <sup>-2</sup> )	Overpotential (mV)	Life (h)	Reference
Ag coating	0.2	0.2	~19	1450	This work
	1	1	~23	350	
	2	2	~26	150	
	5	1	~36	150	
	10	1	~50	100	
mxene	0.2	0.2	~23	800	Angew. Chem. Int. Ed. 2020, 59, 1-6. <sup>1</sup>
CaCO <sub>3</sub> coating	0.25	0.05	~40	840	Adv. Energy Mater. 2018, 8, 1801090. <sup>2</sup>
TiO <sub>2</sub> coating	1	1	~52	150	Adv. Mater. Interfaces 2018, 5, 1800848. <sup>3</sup>
Sc <sub>2</sub> O <sub>3</sub>	1	1	~35	200	Journal of Energy Chemistry 2021, 55, 549-556. <sup>4</sup>
Carbon	1	1	~20	400	Adv. Energy Mater. 2020, 10, 1904215. <sup>5</sup>
Al <sub>2</sub> O <sub>3</sub>	1	1	36.5	500	J. Mater. Chem. A, 2020, 8, 7836-7846. <sup>6</sup>
In coating	0.2	0.2	~27	1500	Small 2020, 16, 2001736. <sup>7</sup>
Au coating	0.25	0.05	~106	2000	ACS Applied Energy Mater. 2019, 2, 6490-6496. <sup>8</sup>
Cu coating	1	0.5	~30	1500	Energy Storage Mater. 2020, 27, 205-211. <sup>9</sup>
C <sub>3</sub> N <sub>4</sub>	2	2	~50	500	Chem. Eng. J. 2021, 403, 126425. <sup>10</sup>
Kaolin coating	4.4	1.1	~70	800	Adv. Funct. Mater. 2020, 30, 2000599. <sup>11</sup>
rGO coating	1	2	~60	200	ACS Appl Mater Interfaces 2018, 10, 25446-25453. <sup>12</sup>
MOF(UiO-66)-PVDF coating	1	0.5	~41	500	ACS Appl. Mater. Interfaces 2019, 11, 32046-3205. <sup>13</sup>

	Current density (mA cm <sup>-2</sup> )	Areal capacity (mA h cm <sup>-2</sup> )	Zn thickness (μm)	Cycles	Adv. Funct. Mater. 2020, 30, 2001263. <sup>14</sup>
Poly (vinyl buyral)	0.5	0.5	~50	2200	Energy Environ. Sci. 2019, 12, 1938- 1949. <sup>15</sup>
Polyamide coating	0.5	0.25	~100	8000	Adv. Funct. Mater. 2020, 2001867. <sup>16</sup>
TiO <sub>2</sub> /PVDF	0.885	0.885	~50	2000	Energy Environ. Sci. 2020, 13, 503- 510. <sup>17</sup>
ZnO-3D coating	5	1.25	~43	500	

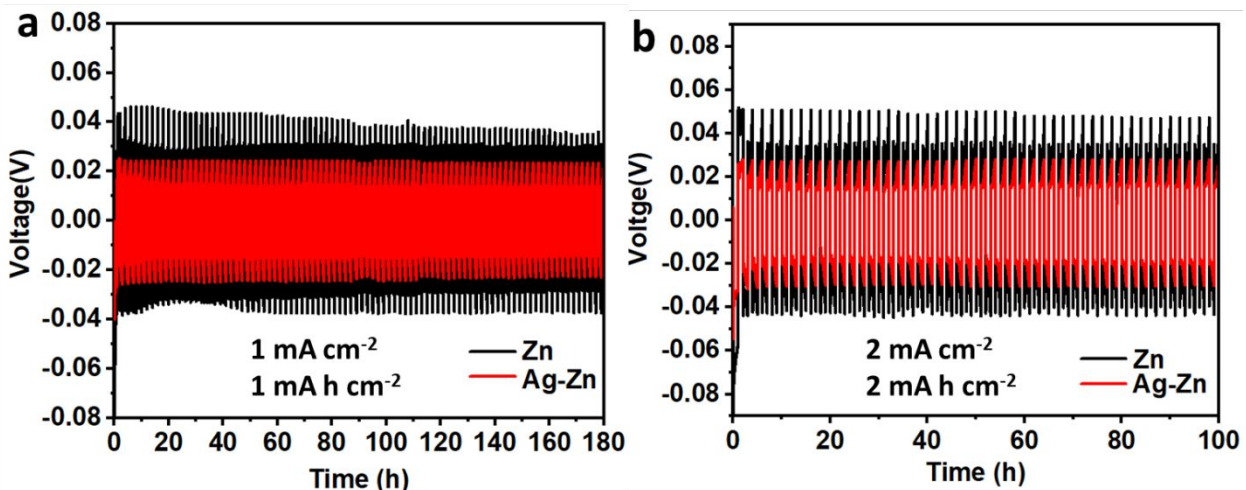


**Figure S7.** Cycling performance of symmetric cells based on Zn foil with 25 μm thickness at current density of a) 1 mA cm<sup>-2</sup> with a capacity of 1 mA h cm<sup>-2</sup> and b) 2 mA cm<sup>-2</sup> with a capacity of 2 mA h cm<sup>-2</sup>.

**Table S2.** Depth of discharge levels of symmetric cells.

Current density (mA cm <sup>-2</sup> )	Areal capacity (mA h cm <sup>-2</sup> )	Zn thickness (μm)	Depth of discharge (%)
2	2	25	14
1	1	25	7
2	2	125	2.8
1	1	125	1.4
0.2	0.2	125	0.28

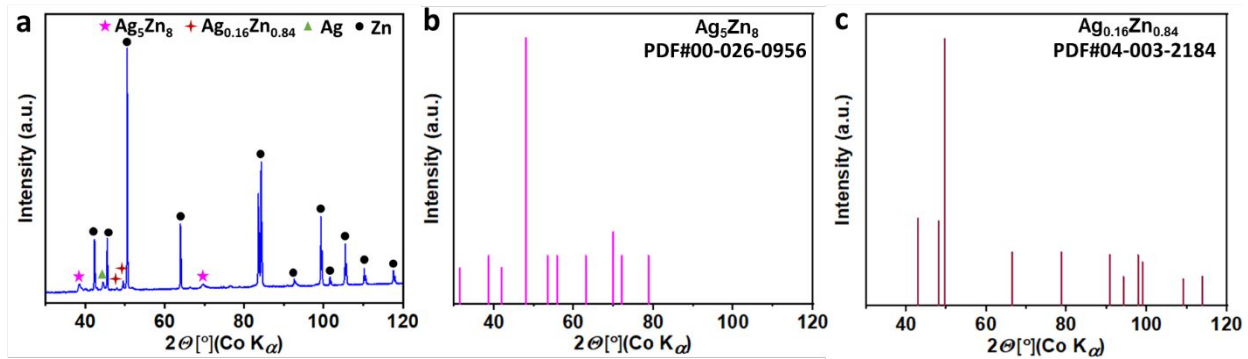


**Figure S8.** a) XRD pattern of Ag-Zn after 1 cycle at a current density of  $0.5 \text{ mA cm}^{-2}$  with a capacity of  $0.25 \text{ mA cm}^{-2}$ . Reference XRD patterns of b)  $\text{Ag}_5\text{Zn}_8$  and c)  $\text{Ag}_{0.16}\text{Zn}_{0.84}$ .

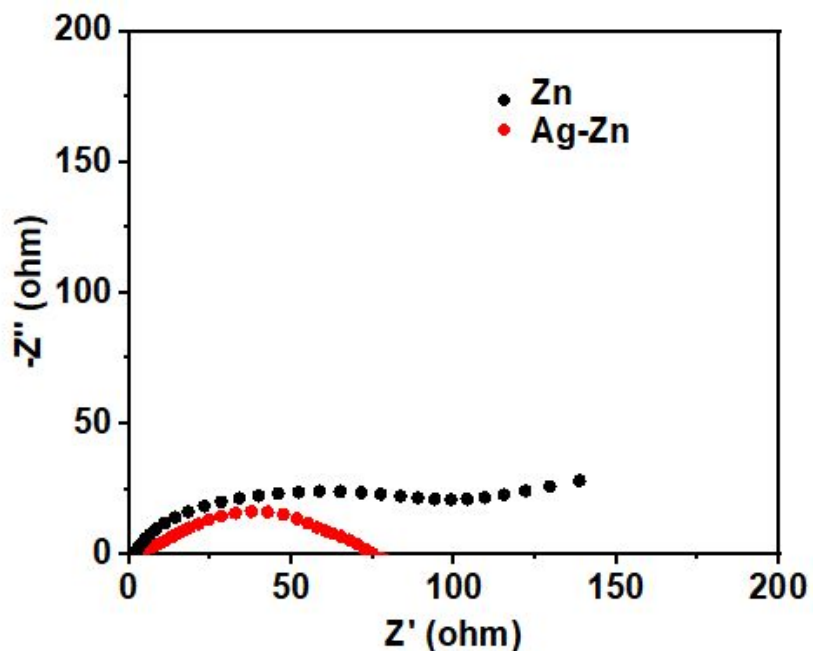


**Figure S9.** Nyquist plot of symmetric cells Zn and Ag-Zn cells.

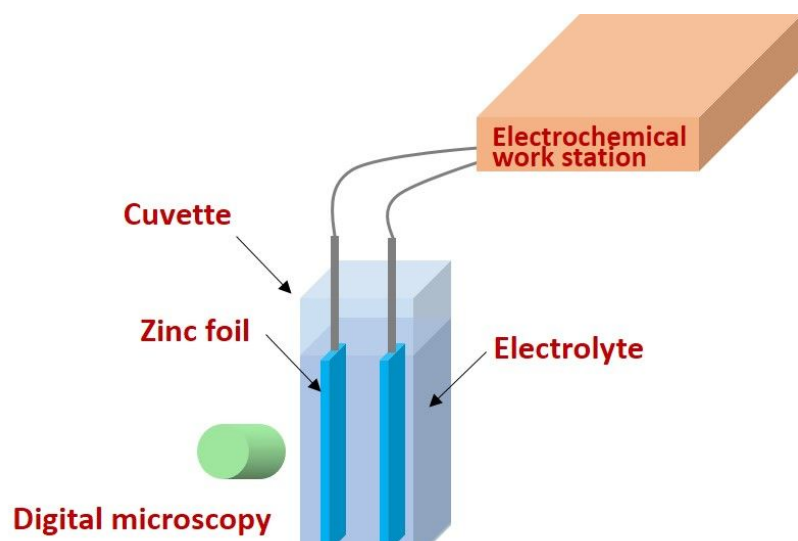


**Figure S10.** Schematic diagram of the set-up for *in situ* microscopy for Zn deposition.

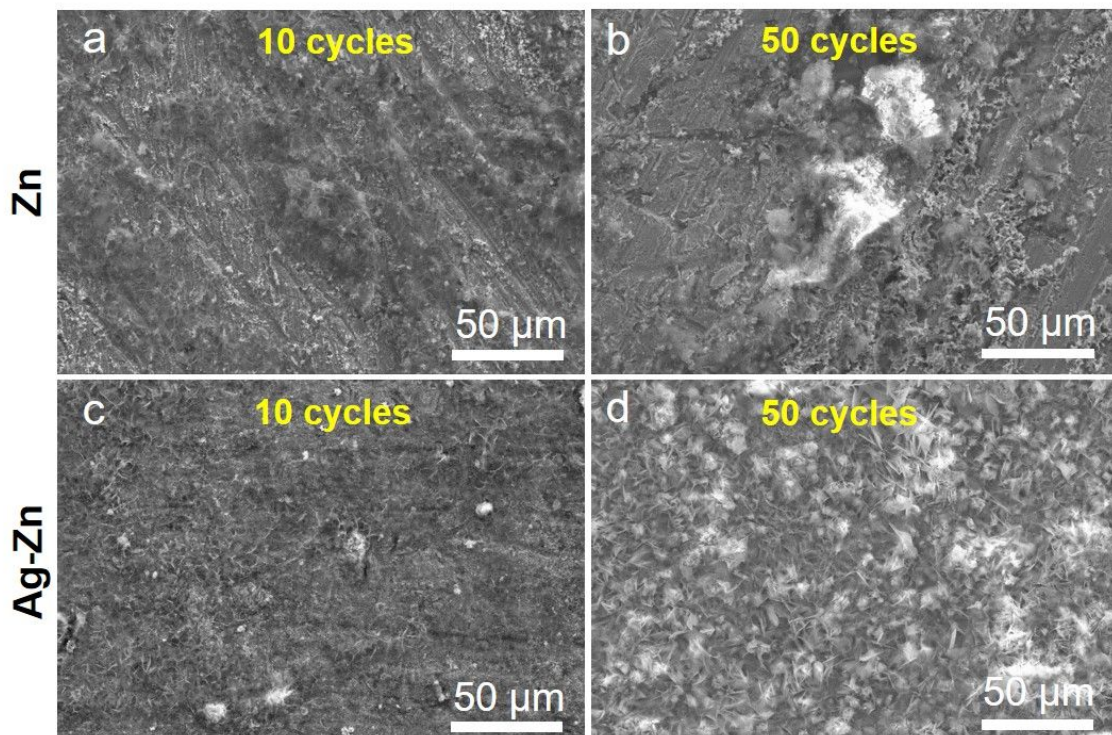


**Figure S11.** SEM images of Zn and Ag-Zn after 10 cycles and 50 cycles at a current density of  $0.25 \text{ mA cm}^{-2}$  with a capacity of  $0.05 \text{ mA h cm}^{-2}$ .

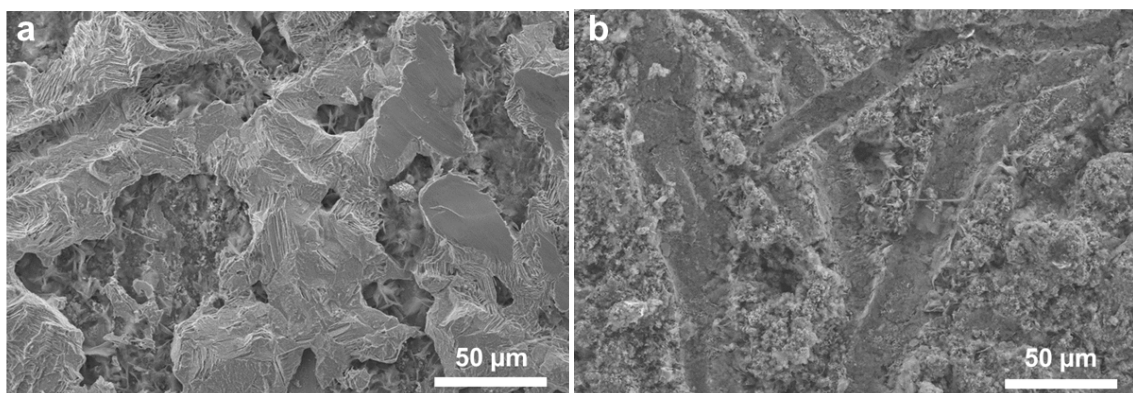


**Figure S12.** SEM images of a) Zn and b) Ag-Zn after 30 cycles at a current density of  $5 \text{ mA cm}^{-2}$  with a capacity of  $1 \text{ mA h cm}^{-2}$ . The grooves in b are due to the fiber of separator.

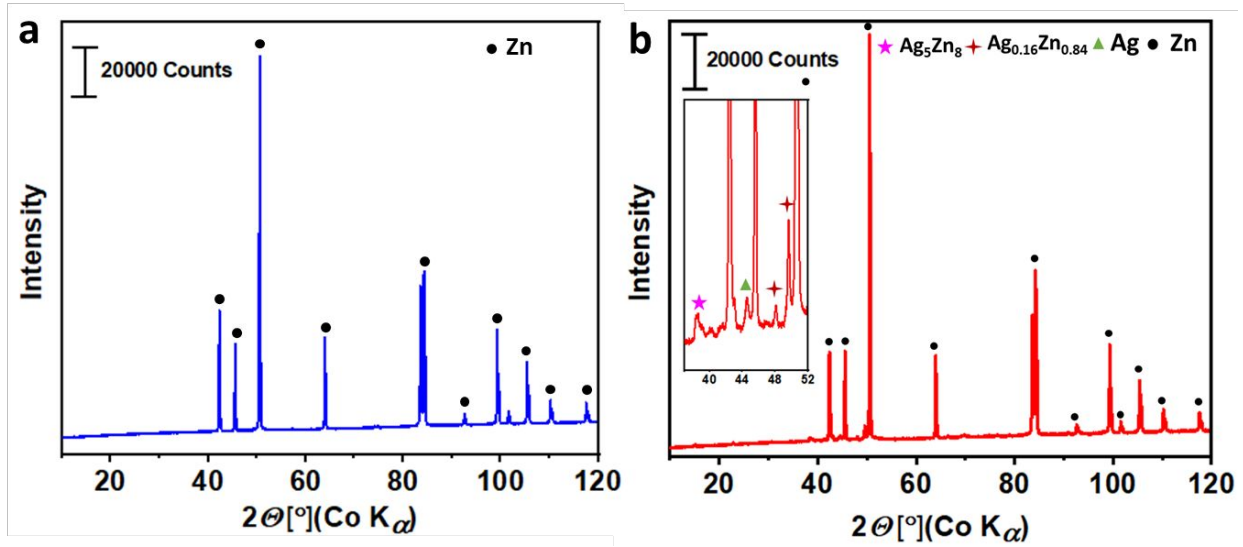


**Figure S13.** XRD pattern of a) Zn and b) Ag-Zn after 30 cycles at a current density of  $5 \text{ mA cm}^{-2}$  with a capacity of  $1 \text{ mA h cm}^{-2}$ .

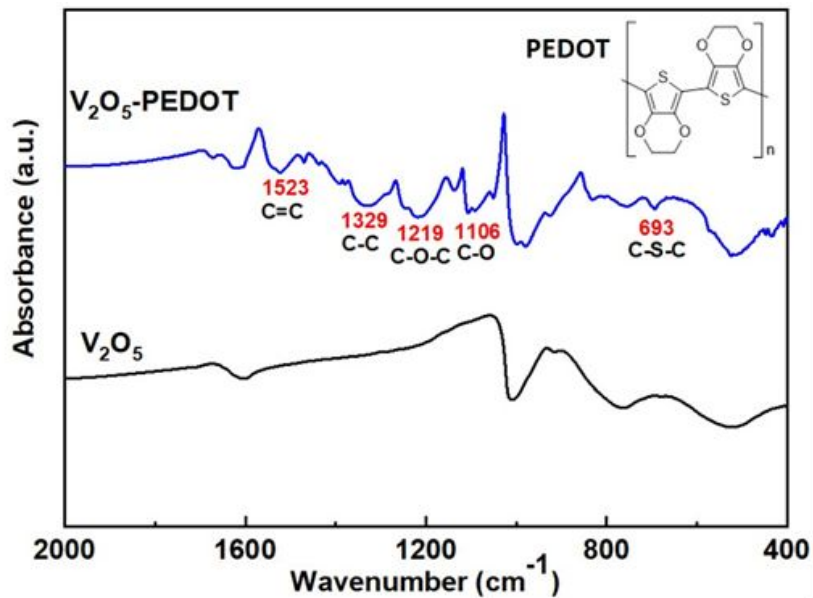


**Figure S14.** FTIR spectra of  $\text{V}_2\text{O}_5$  and  $\text{V}_2\text{O}_5$ -PEDOT, inset represents the molecular structure of PEDOT.

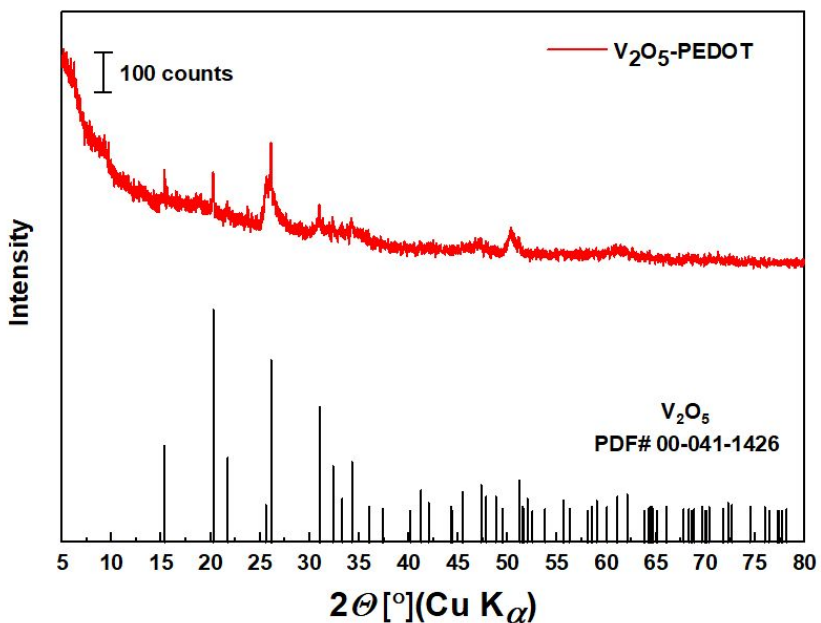


**Figure S15.** XRD pattern of PEDOT-V<sub>2</sub>O<sub>5</sub> composite.

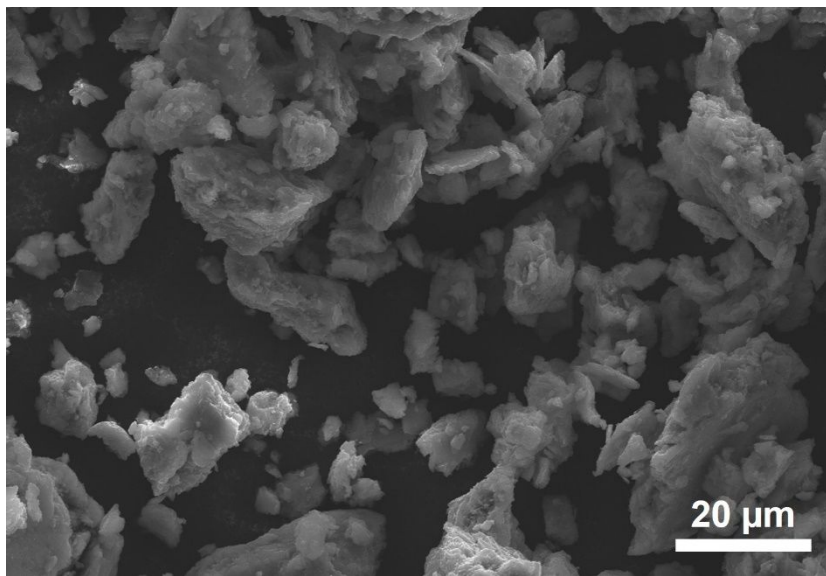


**Figure S16.** SEM image of PEDOT-V<sub>2</sub>O<sub>5</sub> composite.

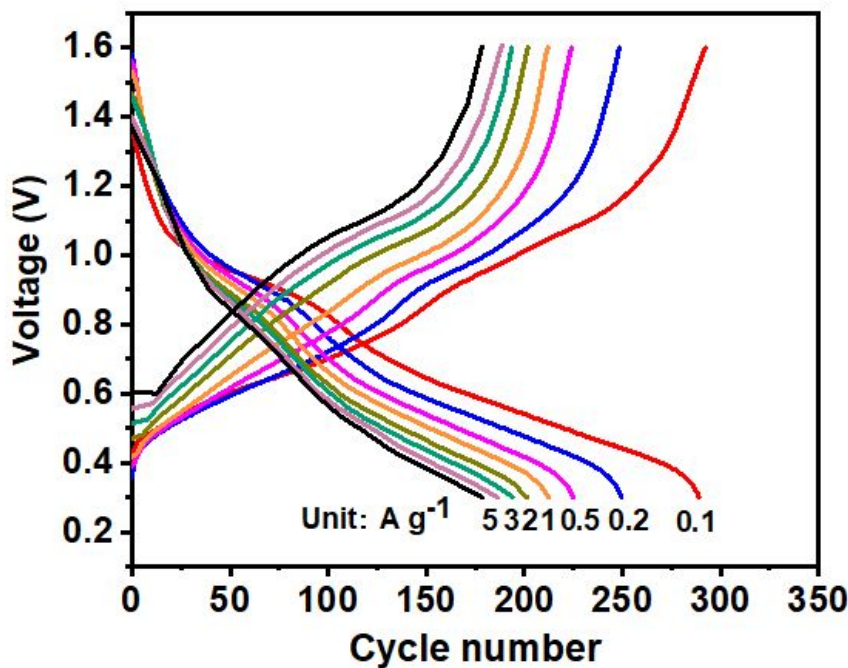


**Figure S17.** Charge/discharge curves of Zn// $\text{V}_2\text{O}_5$ -PEDOT at different current densities.

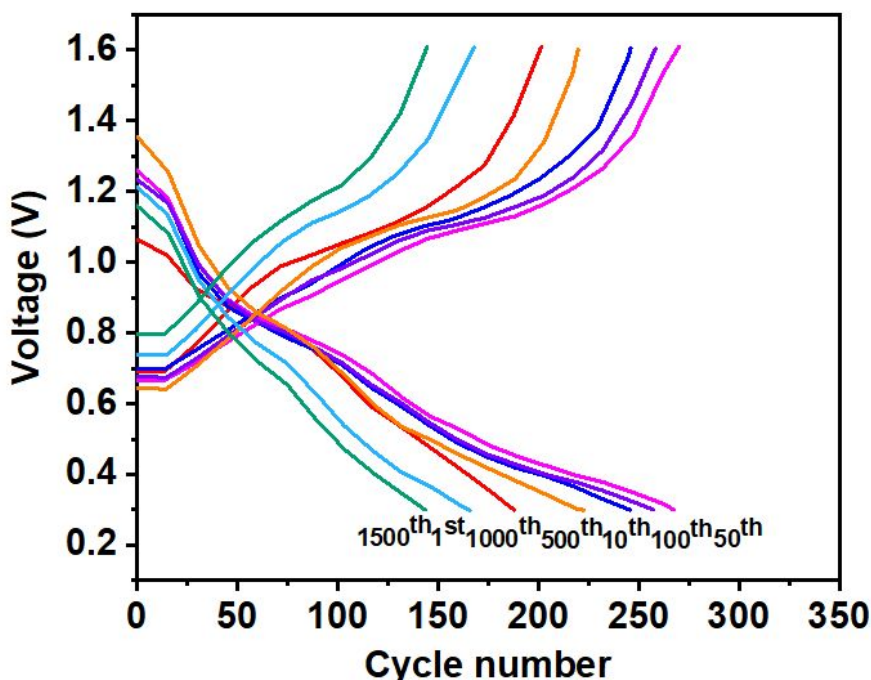


**Figure S18.** Charge/discharge curves of Zn// $\text{V}_2\text{O}_5$ -PEDOT at different cycles at 5  $\text{A g}^{-1}$ .

## References

- (1) Zhang, N.; Huang, S.; Yuan, Z.; Zhu, J.; Zhao, Z.; Niu, Z. Direct Self-Assembly of Mxene on Zn Anodes for Dendrite-Free Aqueous Zinc-Ion Batteries. *Angew. Chem. Int. Ed.* **2020**, *59*, 1-6.
- (2) Kang, L.; Cui, M.; Jiang, F.; Gao, Y.; Luo, H.; Liu, J.; Liang, W.; Zhi, C. Nanoporous Caco<sub>3</sub> Coatings Enabled Uniform Zn Stripping/Plating for Long-Life Zinc Rechargeable Aqueous Batteries. *Adv. Energy Mater.* **2018**, *8*, 1801090.
- (3) Zhao, K.; Wang, C.; Yu, Y.; Yan, M.; Wei, Q.; He, P.; Dong, Y.; Zhang, Z.; Wang, X.; Mai, L. Ultrathin Surface Coating Enables Stabilized Zinc Metal Anode. *Adv. Mater. Inter.* **2018**, *5*, 1800848.
- (4) Zhou, M.; Guo, S.; Fang, G.; Sun, H.; Cao, X.; Zhou, J.; Pan, A.; Liang, S. Suppressing by-Product Via Stratified Adsorption Effect to Assist Highly Reversible Zinc Anode in Aqueous Electrolyte. *Journal of Energy Chemistry* **2021**, *55*, 549-556.
- (5) Yuksel, R.; Buyukcakir, O.; Seong, W. K.; Ruoff, R. S. Metal-Organic Framework Integrated Anodes for Aqueous Zinc-Ion Batteries. *Adv. Energy Mater.* **2020**, *10*, 1904215.
- (6) He, H.; Tong, H.; Song, X.; Song, X.; Liu, J. Highly Stable Zn Metal Anodes Enabled by Atomic Layer Deposited Al<sub>2</sub>O<sub>3</sub> Coating for Aqueous Zinc-Ion Batteries. *J. Mater. Chem.A* **2020**, *8*, 7836-7846.
- (7) Han, D.; Wu, S.; Zhang, S.; Deng, Y.; Cui, C.; Zhang, L.; Long, Y.; Li, H.; Tao, Y.; Weng, Z.; Yang, Q.-H.; Kang, F. A Corrosion-Resistant and Dendrite-Free Zinc Metal Anode in Aqueous Systems. *Small* **2020**, *16*, 2001736.
- (8) Cui, M.; Xiao, Y.; Kang, L.; Du, W.; Gao, Y.; Sun, X.; Zhou, Y.; Li, X.; Li, H.; Jiang, F.; Zhi, C. Quasi-Isolated Au Particles as Heterogeneous Seeds to Guide Uniform Zn Deposition for Aqueous Zinc-Ion Batteries. *ACS Appl. Energy Mater.* **2019**, *2*, 6490-6496.
- (9) Cai, Z.; Ou, Y.; Wang, J.; Xiao, R.; Fu, L.; Yuan, Z.; Zhan, R.; Sun, Y. Chemically Resistant Cu-Zn/Zn Composite Anode for Long Cycling Aqueous Batteries. *Energy Stor. Mater.* **2020**, *27*, 205-211.
- (10) Liu, P.; Zhang, Z.; Hao, R.; Huang, Y.; Liu, W.; Tan, Y.; Li, P.; Yan, J.; Liu, K. Ultra-Highly Stable Zinc Metal Anode Via 3d-Printed G-C<sub>3</sub>n<sub>4</sub> Modulating Interface for Long Life Energy Storage Systems. *Chem. Eng. J.* **2021**, *403*, 126425.
- (11) Deng, C.; Xie, X.; Han, J.; Tang, Y.; Gao, J.; Liu, C.; Shi, X.; Zhou, J.; Liang, S. A Sieve-Functional and Uniform-Porous Kaolin Layer toward Stable Zinc Metal Anode. *Adv. Funct. Mater.* **2020**, *30*, 2000599.
- (12) Shen, C.; Li, X.; Li, N.; Xie, K.; Wang, J.-g.; Liu, X.; Wei, B. Graphene-Boosted, High-Performance Aqueous Zn-Ion Battery. *ACS Appl. Mater. Interfaces* **2018**, *10*, 25446-25453.
- (13) Liu, M.; Yang, L.; Liu, H.; Amine, A.; Zhao, Q.; Song, Y.; Yang, J.; Wang, K.; Pan, F. Artificial Solid-Electrolyte Interface Facilitating Dendrite-Free Zinc Metal Anodes Via Nanowetting Effect. *ACS Appl. Mater. Interfaces* **2019**, *11*, 32046-32051.
- (14) Hao, J.; Li, X.; Zhang, S.; Yang, F.; Zeng, X.; Zhang, S.; Bo, G.; Wang, C.; Guo, Z. Designing Dendrite-Free Zinc Anodes for Advanced Aqueous Zinc Batteries. *Adv. Funct. Mater.* **2020**, *30*, 2001263.
- (15) Dong, Y.; Jia, M.; Wang, Y.; Xu, J.; Liu, Y.; Jiao, L.; Zhang, N. Long-Life Zinc/Vanadium Pentoxide Battery Enabled by a Concentrated Aqueous Znso<sub>4</sub> Electrolyte with Proton and Zinc Ion Co-Intercalation. *ACS Appl. Energy Mater.* **2020**, *3*, 11183-11192.
- (16) Zhao, R.; Yang, Y.; Liu, G.; Zhu, R.; Huang, J.; Chen, Z.; Gao, Z.; Chen, X.; Qie, L. Redirected Zn Electrodeposition by an Anti-Corrosion Elastic Constraint for Highly Reversible Zn Anodes. *Adv. Funct. Mater.* **2021**, *31*, 2001867.
- (17) Xie, X.; Liang, S.; Gao, J.; Guo, S.; Guo, J.; Wang, C.; Xu, G.; Wu, X.; Chen, G.; Zhou, J. Manipulating the Ion-Transfer Kinetics and Interface Stability for High-Performance Zinc Metal Anodes. *Energy Environ. Sci.* **2020**, *13*, 503-510.